Polarization Effects on Thermally Stable Latency in Hollow-Core Photonic Bandgap Fibers

Eric Numkam Fokoua, Wenwu Zhu, Meng Ding, Zitong Feng, Yong Chen, Thomas D. Bradley, Gregory T. Jasion, David J. Richardson, Francesco Poletti, and Radan Slavík

***Abstract*— Conveyance of light in air endows hollow-core optical fibers with remarkably low sensitivity of the propagation delay to temperature changes. This sensitivity was demonstrated to be further reduced and even made negative (crossing zero) in photonic bandgap type of hollow core fibers. When operating long lengths of this fiber close to the zero sensitivity wavelength, it was observed experimentally that there is a small residual variation in propagation delay which had no apparent correlation to imposed temperature changes.**

In this paper, we analyze the polarization effects that give rise to this variation, showing that the highest level of practically achievable thermal stability of the latency is limited by polarization mode dispersion. We show measurements of differential group delay between polarization modes in long lengths of photonic bandgap fiber at various temperatures and focus on spectral regions where thermally stable latency is predicted and measured. Our experimental observations, corroborated by numerical simulations, indicate the presence of strong polarization mode coupling in the fibers in addition to birefringence. The detailed understanding gained through this study allows us to propose practically achievable (i.e., manufacturable) fiber designs with up to three orders of magnitude lower polarization mode dispersion at wavelengths where the latency is insensitive to thermal fluctuations. This paves the way to fibers with polarization independent and thermally stable latency to serve a multitude of applications.

***Index Terms*—Optical Fibers, Hollow-core fibers, Polarization mode dispersion**

I. Introduction

The transit time of an optical signal through a length of optical fiber changes with the environment, most notably with temperature. This change with temperature is quantified by the thermal coefficient of delay (TCD). In a 1 km length of un-cabled standard single mode optical fiber (SSMF), a temperature change of 1 ºC causes ~40 ps change in light propagation time through the fiber (TCD = 40 ps/km/ºC) [1]. This unwanted sensitivity poses significant challenges in a multitude of applications such as the distribution of ultra-precise (sub-ps) timing signals for synchronization purposes in large telescope arrays, phase-arrayed antennae or in large experimental facilities like synchrotrons (e.g., FLASH in Desy, Hamburg) [2, 3]. It also impacts communications applications, for example, in warehouse-scale datacenters where the provision of low and stable latency is emerging as a key requirement for optical switching to become advantageous [4, 5], or in future 5G networks where picosecond-level synchronization between cellular base stations is critical for precise positioning at the centimeter level [6].

In many such applications, the fiber's environmental sensitivity must be monitored and actively compensated, often with complex and costly engineering approaches such as bidirectional signal propagation and active fiber length stabilization [3, 7]. The use of an optical fiber with low or even zero TCD would constitute a passive, simple and elegant solution to such problems. Proposals in this direction include phase stabilized cables which are essentially SSMFs with specialty coatings (with a negative coefficient of thermal expansion to compensate for the refractive index increase due to the thermo-optic effect) [1], or hollow core optical fibers (HCFs) which have TCD values as low as 2 ps/km/ºC (20 times lower than SSMF) [8]. This low TCD in HCFs is a consequence of the reduced overlap between the propagating optical field and the glass material. Thus, guidance in air practically eliminates propagation time variations due to the thermo-optic effect (temperature-induced glass refractive index change), the dominant contributor to the thermal sensitivity in SSMF. Our recent work went a significant step further and showed that the small TCD in photonic bandgap HCFs can be further reduced, made zero (albeit at a single wavelength only), or even negative, through careful design of the interaction of guided light and the glass microstructure [9]. We achieved this by designing the fiber such that the optical mode sees a slightly lower overlap with glass as temperature increases, making it travel faster, thus compensating the fiber elongation. Indeed, to get this effect

Manuscript received xx 2020, revised xx 2020, accepted xx 2020. This work was supported by EPSRC project "Airguide Photonics", under grant EP/P030181/1, Eric Numkam Fokoua is supported by a Royal Academy of Engineering research fellowship, Wenwu Zhu by a Chinese Scholarship Council award, Francesco Poletti gratefully acknowledges an ERC (grant 682724 Lightpipe), Radan Slavík was supported by Royal Academy of Engineering Senior Research Fellowship.

E. Numkam Fokoua (Eric.Numkam-Fokoua@soton.ac.uk), Y. Chen, T. Bradley, M. Ding, Z. Feng, G. T. Jasion, F. Poletti, D.J. Richardson, and R. Slavik are with the Optoelectronics Research Centre, University of Southampton, Southampton SO17 1BJ, UK (R.Slavik@soton.ac.uk).

W. Zhu was with the Optoelectronics Research Centre, University of Southampton, Southampton SO17 1BJ, UK, and with the School of Optoelectronic Engineering and Instrumentation Science, Dalian University of Technology, Dalian 116024, China.

strong enough to counter-balance the fiber elongation, there must be reasonably large (~0.1%) fraction of the guided mode propagating through the glass. This requirement, however, somewhat conflicts with general strategies to reduce the hollow core fiber loss – e.g., the lowest-loss hollow core fibers today (e.g., Nodeless Antiresonant Nested Fiber, NANF, loss of 0.28 dB/km [10]) have significantly lower fraction of guided mode propagating through the glass (< 0.01%) and thus have properties very different to hollow-core photonic bandgap fibers (HC-PBGFs, lowest reported loss of 1.7 dB/km [11]) studied here. Our initial demonstrations of close-to-zero sensitivity HC-PBGFs were performed in short lengths (<10 m) of fiber where we showed 200x lower TCD than SSMFs over an 11-nm bandwidth near the wavelength of 1530 nm [9]. In subsequent experiments, we exploited this property by using kilometer long samples inside an opto-electronic oscillator, showing a very high thermal stability of the oscillator's frequency [12]. Using similar lengths of fiber, we also investigated how low (TCD = 2 ps/km/ ºC) and ultralow (TCD <0.2 ps/km/ ºC) thermal sensitivity HCFs can improve positioning accuracy in emerging 5G telecommunication networks [6]. In this latter study, we observed that when operating HC-PBGF near the zero delay sensitivity wavelength, the propagation time through the fiber drifted by up to 20 ps without any correlation to the imposed temperature change. A similar variation was observed when allowing the input state of polarization to change, indicating that polarization plays an important role in determining the ultimate stability of the propagation delay. Whilst such small delay changes are acceptable in many applications, better stability would allow for a wider application space. Note that a similar polarization-dependent effect is observed even in temperature-compensated SSMF-based timing links, where for the best performance, polarization-maintaining fibers are preferred [13].

In this paper, we investigate how the thermal stability of HC-PBGF operated in the ultralow TCD regime is affected by the polarization properties of the fiber [14]. We experimentally characterize the polarization properties of a 1-km long HC-PBGF by measuring its differential group delay (DGD) and polarization mode dispersion (PMD) under various thermal settings. These experimental results point to the presence of strong polarization mode coupling within the fiber. Using finite element modeling, we calculate both phase and group birefringence of the fiber and obtain an excellent agreement with the measured PMD when we assume strong polarization mode coupling. The understanding gained from experiments and modeling allows us to identify strategies to significantly reduce polarization-dependent propagation delay changes. We discuss these strategies, showing that through improvements in the fiber symmetry, both birefringence and mode coupling can be significantly reduced, potentially resulting in up to three orders of magnitude reduction in polarization mode dispersion. Such fiber designs would provide ultralow and thermally stable latency, representing a passive solution meeting the requirements of the most demanding timing applications.

The paper is organized as follows: In Section II, we present experimental characterization of the polarization properties of the 1km-long, 19-cell HC-PBGF. In Section III, we theoretically analyze the polarization properties of the fiber through finite element simulations of its permittivity profile from a scanning electron micrograph (SEM image). The excellent agreement with experiment validates our model and allows us to explore fiber designs with significantly improved performance which are presented in Section IV, followed by conclusions in Section V.

II. Experimental Assessment of DGD/PMD in Photonic Bandgap HCFs

A SEM image of the cross-section of the fiber used in our experiments is shown in Fig. 1. Its microstructured cladding consists of the typical triangular lattice of air holes embedded in a silica matrix, with 19 unit cells removed to form the core. The fiber was fabricated in-house using a conventional two stage stack and draw method, and was drawn to a length of 1.1 km. It has a core diameter of 31.5 µm, with the microstructured cladding region having nominal diameter of 91 µm. The outer diameter was measured to be 228 µm, and the fiber was further protected with a single layer of UV-curable polymer (DeSolite®3471-3-14) of ~ 40 µm thickness. The fiber loss measured using a cutback method from 1.13 km to 10 m is shown in Fig.1 with a minimum of 4 dB/km near 1520 nm and a transmission window partitioned by two groups of surface modes near 1320 nm and 1440 nm. Also shown in Fig.1, is the TCD of this fiber measured using the method in [12]. The TCD of 1.5 ps/km/ºC at 1550 nm, reduces to 1 ps/km/ºC near 1590 nm, achieves TCD = 0 at 1611 nm, and becomes negative at wavelengths beyond 1611 nm.

We built two set-ups to probe the differential properties between orthogonal polarization states of the fundamental mode and their impact on the thermal sensitivity of the fiber, which are described below in detail. The first one implements the RF phase-shift technique where we measured the relative signal delay through the fiber as a function of the input polarization state and temperature, and the second, commonly referred to as 'fixed analyzer method' allows for direct PMD estimation.

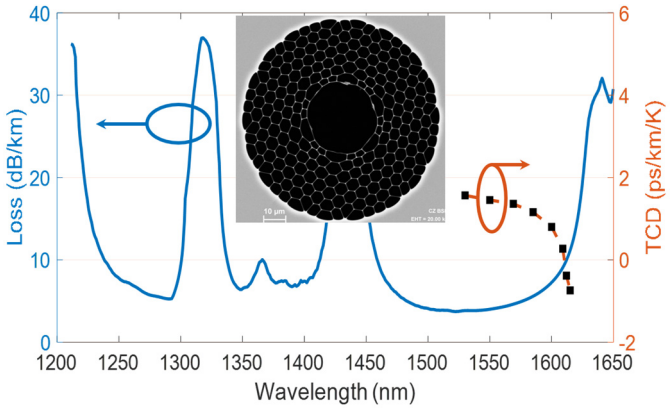

Fig.1: SEM image and measured transmission properties the fiber under test. The blue cure shows the measured loss, whilst the square markers show the measured thermal coefficient of delay (TCD).

A. RF phase shift measurement

The first setup is shown in Fig 2(a). A polarization-maintaining SSMF-coupled tunable laser source (TLS, we used two lasers, a C-band and a L-band, together covering 1520 - 1620 nm) was amplitude modulated with a 7-GHz sine wave

using a Mach-Zehnder modulator (MZM). The modulated signal was sent to a 99:1 splitter with the 1% output fed back into the MZM to keep it at its quadrature point, whilst the 99% output was sent into a polarization controller which was fusion spliced to the fiber under test (FUT) through a suitable mode-field adapter. Care was taken in selecting the mode-field adapter to ensure that only the fundamental modes were excited, with higher order modes extinctions in excess of 20dB. The FUT was placed inside a custom-built thermal chamber and its output spliced to a SSMF using a similar mode-field adapter. This sealed the FUT (to prevent dust and moisture ingress), but also acted as a modal filter to eliminate the parasitic optical power carried by the FUT's lossy higher-order modes. After photodetection, the 7-GHz sine wave signal was visualized with an oscilloscope, together with the original 7-GHz modulating sine wave. This allowed us to record the RF phase delay as the input state of polarization was changed and for various temperature settings of the thermal chamber. After each temperature settings of the thermal chamber had stabilized, we recorded the maximum and minimum RF phases as input polarization was changed and used this to calculate the DGD, i.e. the difference in propagation time between the fastest and the slowest mode.

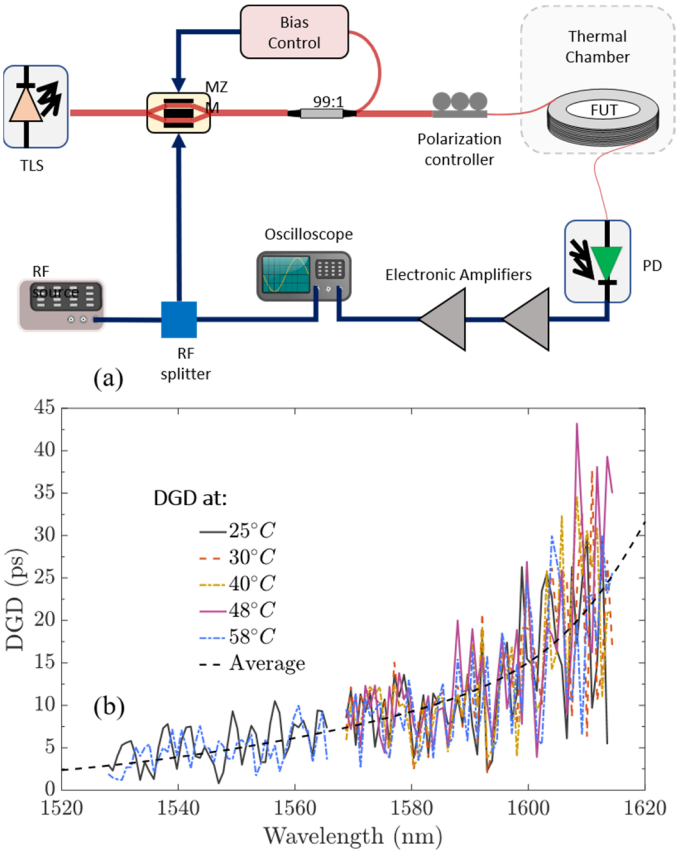

Fig.2: (a) Experimental Setup for DGD using the time-of-flight technique. TLS: tunable laser source, MZM: Mach-Zehnder modulator, FUT: Fiber under test, PD: photodiode (b) Measured differential group delay as a function of wavelength (measured with the C-band TLS and subsequently with the L-band TLS) and temperature in a 1-km HC-PBGF.

The measured DGD at 25, 30, 40, 48, and 58 ºC are shown in Fig. 2(b) and displays the signature stochastic behavior which attests to strong mode coupling [15]. Its average at each wavelength (defined as the PMD), increases with wavelength as we approach the edge of the photonic bandgap, but is nearly identical for each temperature. Near 1610 nm, where we measured zero TCD, the DGD was between 6 and 30 ps, with average value (PMD) of 21 ps, more than five times higher than in the middle of the transmission window (3.8 ps at 1540 nm). Through changing the input polarization state, there can be as much as a 24 ps delay difference through the fiber and this variation has no fixed correlation to the temperature.

Phenomenologically, when the fiber's temperature is changed, the propagation time through it will be influenced by two effects. The first is the thermally-induced propagation time change characterized by the TCD and the other one is related to thermally-induced changes of the principle states of polarization. Considering TCD of 2 ps/km/ºC, the fiber's temperature must be changed by as much as 12 ºC to make the thermally-induced delay change as large as that due to the polarization effects. Thus, for small temperature variations (less than 12 ºC), polarization effects represent the dominant contribution to the delay instability. These measurements, in excellent agreement with our previous observations [6], confirm that the presence of PMD represents a significant degradation of the thermal stability of the propagation time in the fiber when operated near its zero TCD point.

B. Fixed analyzer measurement

To corroborate the DGD measurements and obtain further insight into the key drivers of PMD in the FUT, we performed PMD measurements using the *fixed analyzer* method with the setup shown in Fig. 3(a). Here, we injected the polarized output of a supercontinuum broadband source into the FUT which remained in the thermal chamber (Fig. 3). Its output went through a fiber polarizer before being collected by an optical spectrum analyzer (resolution of 0.01 nm). We recorded the spectrally random intensity distribution (Fig. 3(b) shows an example of a recorded trace) at 20, 30, 40, and 50 ºC, waiting a few hours each time for the chamber's temperature to stabilize. This data was then processed by counting the extrema in the spectral intensity curve [16] to obtain PMD shown in Fig. 3(c) at all four temperature settings.

Apart from the very edge of the bandgap where they diverge, the PMD values obtained with the fixed analyzer setup and the measurement results obtained with the phase shift technique agree remarkably well. They show that the relatively low PMD near the center of the transmission window increases rapidly towards the edge of the window where low thermal delay sensitivity occurs. Over the 30 ºC excursion (from 20 to 50), the PMD shows very little change with temperature. In what follows, we further elaborate on the interpretation of the results and comparison with the RF domain measurement.

C. Discussion

As in any optical fiber, the PMD is governed by the interplay between birefringence which in a hollow core fiber is largely determined by the symmetry/asymmetry in the fiber cross-

section, and polarization mode coupling which arises because of local perturbations along the fiber length. The stochastic

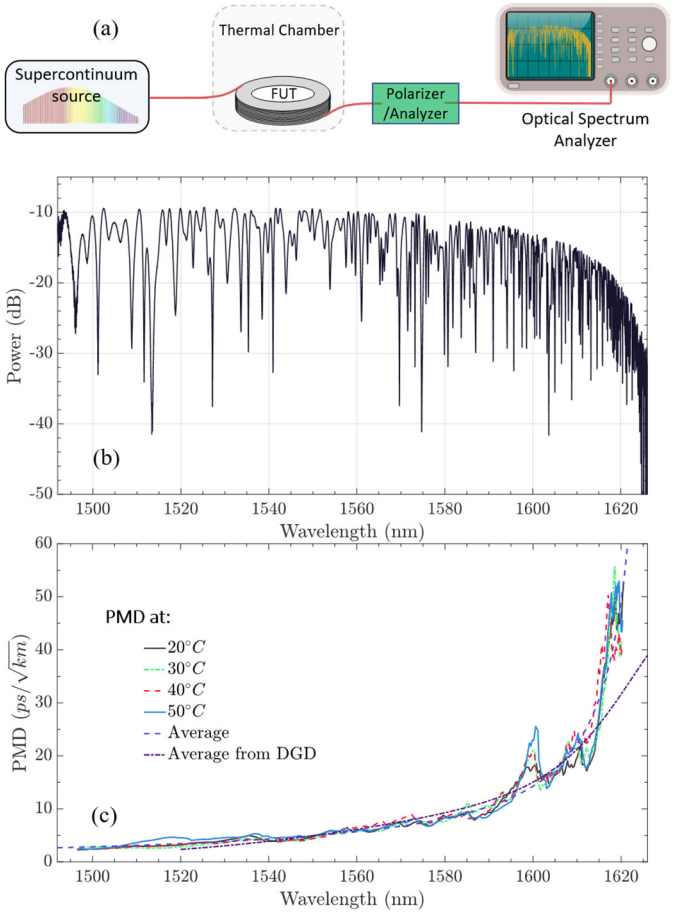

Fig. 3: Fixed analyzer setup (a), example (at 20 ºC) of recorded spectral trace (b), and PMD curves (c) extracted from spectral traces obtained at temperatures of 20, 30, 40, and 50 ºC.

nature of the measured DGD in Fig. 2(b) and the intensity distribution with wavelength in Fig. 3(b) are a clear indication of polarization mode coupling. In the absence of such mode coupling, the DGD would be deterministic and the intensity distribution would show regular beating fringes. Both measurement methods show that for our FUT, the PMD coefficient is ~ 21 $ps/\sqrt{km}$ near 1610 nm where the TCD is near zero. In contrast, it is lower near the center of the transmission window (~3$ps/\sqrt{km}$ at 1530 nm). Interestingly, over the range of temperatures investigated, neither the spread of the DGD values from the RF phase shift measurements, nor the PMD show a significant dependence on temperature.

In the following section, we provide a theoretical analysis into the contributions to PMD. First, we use finite element simulations to calculate the birefringence properties induced by the asymmetries in the cross section. Although the structural variations along the fiber length are difficult to determine, we make reasonable assumption on such variations and employ coupled mode theory to estimate the resulting polarization mode dispersion.

III. Modeling

To model the FUT's properties, we use a fully-vectorial finite element solver (COMSOL Multiphysics) on a permittivity profile obtained from an SEM image of the fiber end-face using the method described in [17]. The accuracy of this modelling procedure is attested by the excellent agreement between the simulated and measured transmission window, spectral position of the surface modes and attenuation, as shown in Fig. 4. It can be appreciated from the inset that these surface modes are supported in the thicker sections of the core boundary. We expect the resulting anti-crossing events, as well as those near the edges of the transmission window to induce differential properties between polarization modes of the fiber [18].

Although HC-PBGFs are inherently multimoded, we consider only fundamental mode properties in our analysis. This is well justified by the fact that in all experimental works on low thermally-sensitive hollow core fibers, HC-PBGFs were operated in single-mode regime by controlling the launch condition (launching predominantly into the fundamental mode) and output condition (always interconnecting HC-PBGF with SSMF first before detection, filtering out higher-order mode content at the HC-PBGF output. Furthermore, the significantly larger differential delay between the fundamental and higher order modes would require very strong intermodal coupling to affect the delay dynamics.

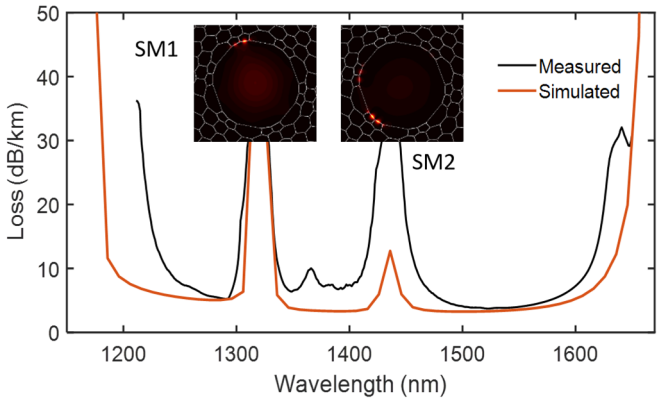

Fig. 4: Comparison of measured (solid black) and simulated (using finite element modeling, red) transmission loss of our FUT.

A. Birefringence properties

We start by calculating the fiber birefringence, focusing on the wide surface mode free region between 1450 and 1650 nm, which covers the minimum loss and ultra-low TCD spectral regions. The asymmetries in the FUT's cross-section and the slight ellipticity of its core break the degeneracy of the fundamental modes and introduce orthogonal linear birefringent axes. Fig. 5 shows the resulting calculated phase Δn_{eff} and group Δn_g birefringence. Our simulations show $\Delta n_{eff} = 3.9 \times 10^{-6}$ and 6.9×10^{-6} at 1550 and 1610 nm respectively (corresponding to ~40 and 23 cm beat lengths respectively). This level of phase birefringence is nearly two orders of magnitude larger than in a typical SSMFs (beat length ~30 m) and about two orders of magnitude lower than in typical polarization-maintaining fiber (beat length ~1-5 mm).

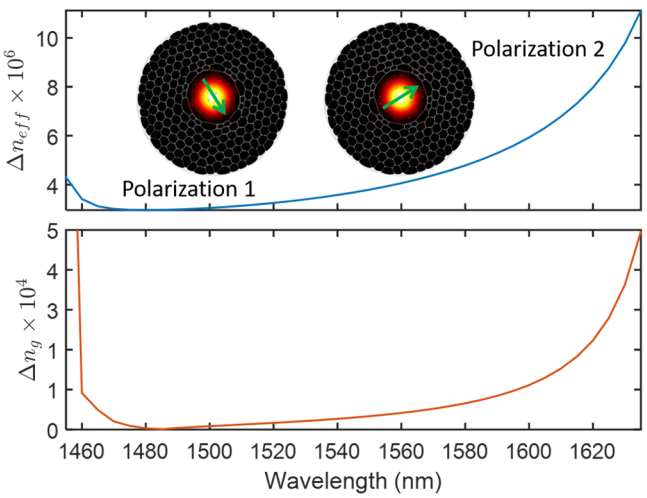

Fig. 5: Simulated phase and group birefringence of FUT.

The corresponding group birefringence is 3.3×10^{-5} and 1.5×10^{-4} at 1550 nm and 1610 nm respectively, more than an order of magnitude larger than the phase birefringence. This is markedly different from the typical behavior found in SSMF or solid-core polarization maintaining fibers, where Δn_{eff} and Δn_g are nearly equal [20]. The simulated birefringence increases rapidly towards the edges of the transmission window, which we associate with the increased overlap of the mode field with the glass material in the vicinity of the anti-crossing events. Near such events, the boundary conditions at the air-glass interfaces that must be satisfied by the optical field polarized along either axis leads to the split in the propagation constants.

B. *Thermal sensitivity*

Using the perturbation approach presented in [9], we calculated the TCD for both polarization modes and show the results in Fig. 6(a). The TCD curves for both polarizations cross

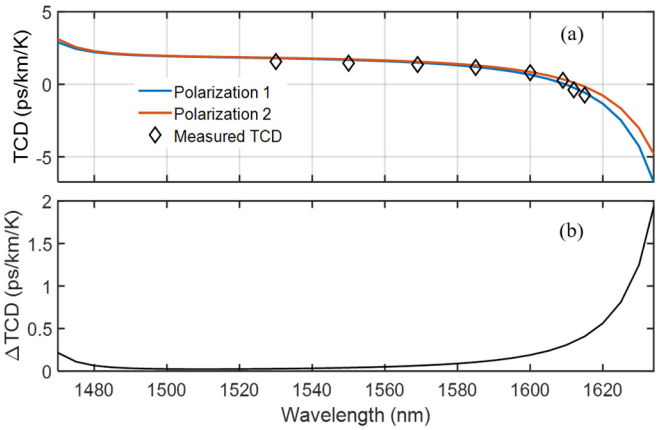

Fig. 6: Simulated TCD for light propagating along two principal polarization axes with measured values shown for comparison (a) and difference between TCDs measured along the two principal polarization axes (b).

zero at 1610 nm and 1613 nm respectively, in good agreement with measurements. The differential TCD (in other words the thermal sensitivity of the DGD in the absence of mode coupling) is plotted for clarity in Fig. 6(b). Near 1610 nm, it amounts to approximately 0.25 ps/km/ °C, while it is about 10 times lower at 1530 nm.

C. *Impact of mode coupling*

At the wavelength of 1610 nm, the group birefringence leads to a normalized DGD $d\tau = \Delta n_g / c$ of 0.5 ps/m. This suggests that in the absence of mode coupling (i.e. the fiber holds polarization and the principal states of polarization are the two orthogonal linear states), the stochastic behavior of the data in Fig. 2 would be absent, and the differential delay (which would scale linearly with the length) would be as high as 500 ps for our 1 km sample as opposed to the measured 21 ps. In this case however, light coupled in either the fast or slow axis would possess thermally stable travel time at their respective zero-TCD wavelengths, which is not what we observed experimentally. This clearly implies that the polarization modes within the fiber are coupled. In the presence of strong coupling, the DGD for a fiber of length L follows a Maxwellian distribution with mean $\langle \Delta\tau \rangle$ and standard deviation σ given by [20-22]:

$$\langle \Delta\tau \rangle = d\tau \sqrt{\frac{8}{\pi} \frac{L}{h}} \qquad (2)$$

$$\sigma = d\tau \sqrt{\left(3 - \frac{8}{\pi}\right) \frac{L}{h}} \qquad (3)$$

where $d\tau = \frac{\Delta n_g}{c}$ is the birefringence-driven DGD per unit length (in s/m) in the absence of any perturbation and $1/h$ represents a mean coupling length. As has been shown extensively, any sufficiently random mode coupling perturbation model leads to the same Maxwellian distribution of the DGD [21]. Of the many possible perturbations that can cause coupling among the polarization modes, we consider here for simplicity that it originates from random shifts of the air-glass interfaces along the fiber length, with this random perturbation obeying a stationary Gaussian process. This is equivalent to fixed birefringence axes but randomly varying magnitude birefringence along the length of the fiber. The coupling length is then estimated as described in the appendix.

Fig. 7(a) shows the calculated mean coupling length as a function of wavelength, with shorter coupling lengths near the edges of the transmission window indicating stronger mode coupling. This is slightly counterintuitive since birefringence is also higher near the edges of the window but shows that the degree to which birefringence prevents mode coupling depends critically on the strength of the overlap between the modes and the perturbed boundaries. Indeed, near the edges of the photonic bandgap or in the vicinity of surface modes, the optical fields overlap more strongly with the glass material and its interfaces, leading to stronger coupling despite higher birefringence.

The resulting mean DGD $\langle \Delta\tau \rangle$ as a function of wavelength is plotted in Fig. 7(b), with the patched area showing the 2σ range for the DGD. We have superimposed measured data from Fig. 2 at room temperature (25 °C) and 48 °C, showing that our

model's assumptions yield a good agreement with experiments.

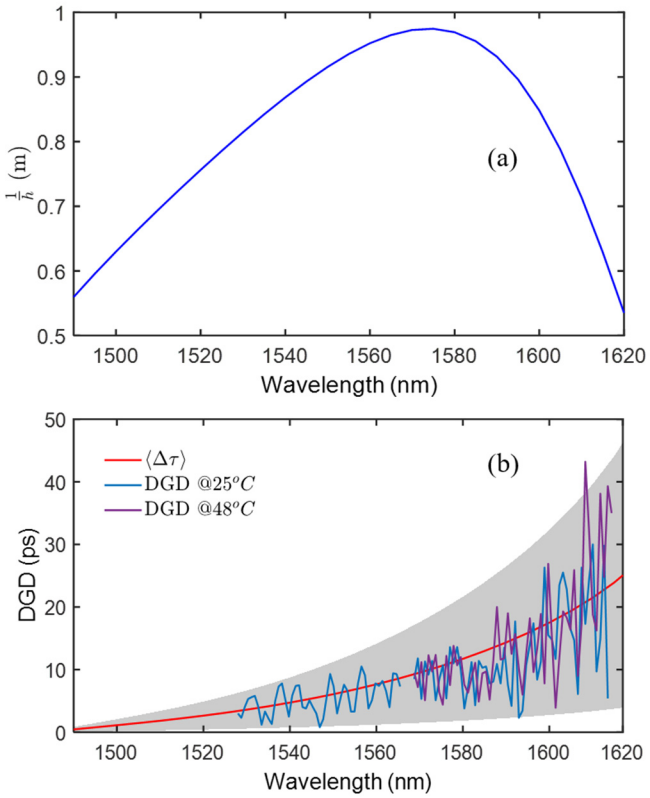

Fig. 7: Modelled coupling length and mean DGD in the 1 km HC-PBGF. The coupling length are calculated as described in the appendix.

These modelling results, together with the experimental observations, which they corroborate very well, confirm birefringence and strong mode-coupling within the fiber as key drivers of the random delay variation within the ultralow thermal sensitivity range.

In conclusion, for ultrastable latency (i.e., >200x better than SMFs), in addition to targeting fiber designs offering TCD = 0 at reasonably low-loss wavelengths, careful fiber design must also aim to minimize the DGD between polarization modes or alternatively, induce even stronger coupling between polarization modes.

IV. Improved Fiber Designs

Because the HC-PBGFs derive their optical properties from the arrangement of their cross-section, careful control of their geometrical parameters can be leveraged to sculpt their polarization properties and their influence on the fiber thermal sensitivity. Based on our analysis above, there are three potential approaches. The first consists of imposing sufficiently high birefringence to eliminate polarization mode coupling (essentially, making the fiber 'polarization maintaining'). Such birefringence can be achieved by deliberately breaking the symmetry of the fiber structure, particularly that of the core surround. Examples include incorporating antiresonant elements in the core surround [23], elliptical core shapes [24] or control of the thickness of the core surround membrane [18, 25]. However, these approaches have so far resulted in more complex structures which support multiple surface modes that reduce the available transmission bandwidth and may result in light at the zero TCD wavelength suffering very high loss.

The second alternative is to induce even stronger polarization mode coupling than apparently present in the fiber. With such strong coupling, Eq. (2) and (3) indicate that both $\langle\Delta\tau\rangle$ and $\sigma \to 0$. In SSMFs, this may be achieved by spinning the fiber preform during fiber draw. Recent reports indicate that this approach may be effective in reducing the PMD in HC-PBGFs, with a twist period of about 1cm reducing the PMD by a factor of 5x to 10x in the middle of the photonic bandgap. However, the thermal response of the fiber/cable was not investigated, and this level of twist does not appear to be effective near the edges of the photonic bandgap [26].

The final alternative is that of designing fibers with as little birefringence as possible. This can be achieved by preserving the six-fold symmetry of the core and fiber structure which will eliminate any birefringence between the two polarization modes [27]. Although challenging, fluid dynamics modelling indicates that such a symmetric structure could be manufactured but would require extremely precise pressure controls during the fiber draw, which are yet to be achieved [28,29]. To illustrate the performance improvements from this approach, we consider the fiber cross-section shown in Fig 8. It has the same core, microstructure, silica glass jacket, and coating diameters as the fiber used in our experiments (the latter is important since coatings affect the fiber's thermal elongation and TCD, see [9]). The key differences are its slightly higher air-filling fraction, increased size of glass nodes on the core boundary and most importantly its improved symmetry which removes the surface modes and widen the transmission window. Fig. 8(a) plots the simulated TCD, showing that the fiber achieves zero TCD near 1650 nm and ultra-low delay sensitivity (TCD < 0.2 ps/km/ °C) over a 7 nm bandwidth. At 1650 nm, the calculated group birefringence is only 3×10^{-8}, more than three orders of magnitude lower than the fabricated fiber. Without mode-coupling, this would lead to a DGD as low as 0.1 ps/km. By considering that the fiber is subject to mode coupling originating from the same perturbation as before, we obtain the mean DGD and its 2σ range as shown in Fig. 8(b), with a value of only $\sim 10\ fs/\sqrt{km}$ at 1650 nm. This means that when operating this improved fiber at its TCD = 0 point, allowing the input polarization states to change would only result in a delay change of only 10 fs. In a fiber with a TCD of 2 ps/km/°C, this is equivalent to as little as a 5 mK temperature change, a level of stability that would meet the needs of the most demanding applications. Clearly, reducing polarization dispersion to such levels would benefit many applications too, in particular telecommunications where PMD can limit the data rates.

Despite virtual fiber draws indicating that this highly symmetric fiber structure can be fabricated, we expect to see some level of asymmetry in real samples. We probed the impact of residual asymmetries by simulating the same fiber with the glass nodes around the core boundary out of position by a factor of 10% and adjusting the wall thickness accordingly through mass conservation. This increased the group birefringence to

7×10^{-6} at the zero sensitivity wavelength, which would lead, under the same mode coupling perturbation, to a mean DGD of 1 ps/km. This would represent more than an order of magnitude improvement over the current fiber, a latency stability level adequate for a large range of applications.

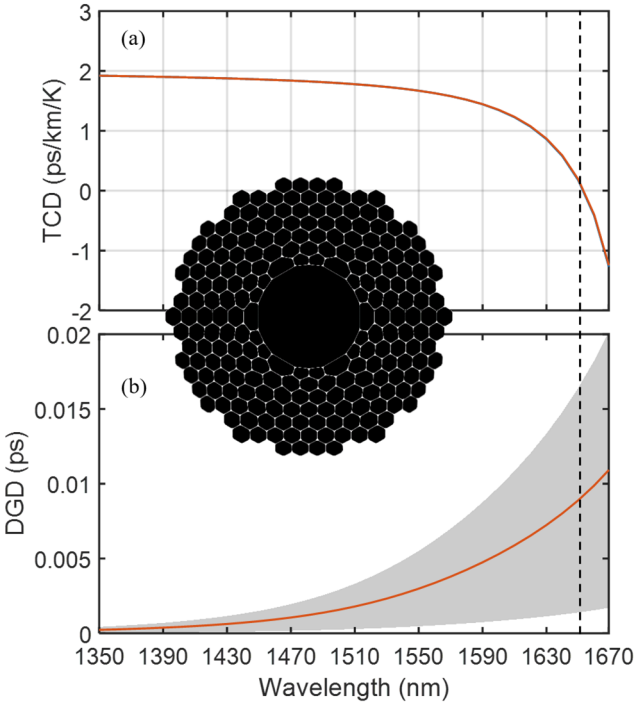

Fig. 8: Thermal coefficient of delay (a) and DGD and PMD in an improved 19-cell HC-PBGF design with six-fold symmetry. The DGD (the patched area shows its 2σ range) and PMD (red, solid line) are calculated for 1 km of fiber under the strong coupling assumption.

V. Conclusion

We have analyzed experimentally and theoretically, the impact of polarization on the thermal stability of the propagation delay in a kilometer-long 19 cell HC-PBGF. Using accurate finite element simulations, we showed that small structural asymmetries in the fiber cross-section result in phase and group birefringence that grow larger towards the bandgap edges. Near these edges, the strong mode field overlap with the glass results in strong mode-coupling despite the birefringence. These two effects combine to give a significant polarization mode dispersion at the bandgap edge. At the zero delay thermal sensitivity wavelength (which occurs at the long wavelength bandgap edge), the high stability of latency is ultimately limited by the PMD. We discuss methods to reduce the PMD, showing that highly symmetric but potentially achievable structures with improved symmetry can dramatically reduce the PMD by up to 3 orders of magnitude, paving way for ultralow, polarization and temperature-insensitive latency.

It is worth mentioning that recently developed hollow-core fibres based on anti-resonant guiding (rather than photonic bandgap guidance) simultaneously offer low loss, low birefringence, and low levels of polarization mode coupling [10, 30] (making them ideal for applications like telecom or high-power transmission). However, they carry very little optical power in the glass making it difficult to tailor their dispersion and thermal sensitivity which remains limited by elongation, but still 20x lower than in SSMFs. HC-PBGFs are therefore uniquely suited for the many applications where ultra-stable latency (thermal sensitivities better than 200x lower than SSMFs) is more important than loss.

VI. Appendix

In the presence of longitudinal perturbations along the length of the fiber, the coupling length between polarization modes of HC-PBGFs can be estimated by means of coupled mode theory [31, 32]. For stochastic perturbations, we are interested in the evolution of the ensemble average modal intensities P_m for mode m which under very general assumptions obeys [32]:

$$\frac{\partial P_m(z)}{\partial z} = -\alpha_m P_m(z) + \sum_{n \neq m} h_{mn}\big(P_n(z) - P_m(z)\big), \quad (A1)$$

where α_m is the loss of mode m and h_{nm} is the power coupling coefficient between the two modes m and n [29]. Many plausible sources of perturbations could give rise to coupling between polarization modes, for example slow random twists, random core size fluctuations, etc. As these are all difficult to measure experimentally, here, without loss of generality, we consider that the perturbations in HC-PBGFs amount to the shifting of the interfaces between air and glass by a small, stochastic and zero-mean amount $f(s,z)$ (where s is a curvilinear coordinate along an air-hole in the cross-section). If we further assume that the correlation length of the perturbation along s is significantly longer than the perimeter of the air-holes within the fiber so that only the dependence with z matters, the power coupling coefficients take the form:

$$h_{mn} = |\kappa_{mn}|^2 \Psi(\beta_m - \beta_n)\,. \quad (A2)$$

Here, Ψ is the power spectrum of the perturbations, and the modal overlap κ_{mn} from coupled mode theory is:

$$|\kappa_{mn}|^2 = \sum_{air\ holes} \left| \frac{\omega \varepsilon_0}{4} \oint \left[(n^2 - 1) \boldsymbol{E}^*_{m\parallel} \cdot \boldsymbol{E}_{n\parallel} - \left(\frac{1}{n^2} - 1\right) \boldsymbol{D}^*_{m\perp} \cdot \boldsymbol{D}_{n\perp} \right] dxdy \right|^2 . \quad (A3)$$

The subscripts $\parallel$ and $\perp$ refer to field components parallel and orthogonal to the boundaries, ensuring that all quantities entering the calculation are continuous across the interface [33]. If the spectrum Ψ is known, one uses Eq. (A2) and (A3) to calculate the coupling length that enters Eq. (2) and (3) with m and n being the orthogonal polarizations of the fundamental mode.

The exact nature of the perturbations that cause polarization mode coupling is not known and is difficult to assess experimentally. Roberts [23] argues that the intrinsic surface roughness from frozen-in surface capillary waves may play an important role in coupling polarization modes of HC-PBGFs, however, this intrinsic surface roughness at length scales similar to the birefringence (~10s of cm) in HC-PBGFs is yet to be measured experimentally. To obtain the coupling length data

plotted in Fig. 7(a), we speculate that the power spectrum of interests is that of a stationary Gaussian distribution with 10 nm root mean square (rms) value and a correlation length of 1 cm. Although the calculated mode dispersion with this assumption match our experiments, the nature of perturbations that gives rise to such mode coupling in HC-PBGFs is yet to be fully understood.

REFERENCES

[1] M. Bousonville, M. K. Bock, M. Felber, T. Ladwig, T. Lamb, H. Schlarb, S. Schulz, C. Sydlo, "New phase stable optical fiber," Proc. of Beam Instrumentation Workshop (BIW 2012), paper MOPG033, 101, Newport News, VA, USA, April 15-19, 2012.

[2] F. Loehl, V. Arsov, M. Felber, K. Hacker, B. Lorbeer, F. Ludwig, K. Matthiesen, H. Schlarb, B. Schmidt, A. Winter, S. Schulz, J. Zemella, J. Szewinski, W. Jalmuzna, "Measurement and stabilization of the bunch arrival time at FLASH," Proceedings of the 11th European Particle Accelerator Conference (EPAC'08), paper THCP158, pp. 3360-3362, Genoa, Italy, 2008.

[3] G. Grosche, O. Terra, K. Predehl, R. Holzwarth, B. Lipphardt, F. Vogt, U. Sterr, and H. Schnatz, "Optical frequency transfer via 146 km fiber link with 10^{-19} relative accuracy," Opt. Lett. 34, 2270 (2009).

[4] H. Ballani, P. Costa, I. Haller, K. Jozwik, K. Shi, B. Thomsen, and H. Williams, "Bridging the Last Mile for Optical Switching in Data Centers," Proc OFC 2018

[5] K. A. Clark, Y. Chen, E. R. Numkam Fokoua, T. Bradley, F. Poletti, D. J. Richardson, P. Bayvel, Slavík and Z. Liu, "Low Thermal Sensitivity Hollow Core Fiber for Optically-Switched Data Centers," *accepted for publication* in J. Ligthw. Technol 2020

[6] W. Zhu, E. Numkam Fokoua, Y. Chen, T. Bradley, S. R. Sandoghchi, M. Ding, G. T. Jasion, M. N. Petrovich, F. Poletti, M. Zhao, D. J. Richardson, and R. Slavík, "Toward High Accuracy Positioning in 5G via Passive Synchronization of Base Stations Using Thermally-Insensitive Optical Fibers," in IEEE Access 7, 113197-113205, 2019.

[7] C. Lisdat, G. Grosche, N. Quintin et al., "A clock network for geodesy and fundamental science", Nat. Commun. 7, 12443 (2016)

[8] R. Slavík, G. Marra, E. Numkam Kokoua, N. Baddela, N.V. Wheeler, M. Petrovich, F. Poletti, and D.J. Richardson, "Ultralow thermal sensitivity of phase and propagation delay in hollow core optical fibers, " Sci. Rep. 5, 15447 (2015).

[9] E. Numkam Fokoua, M. N. Petrovich, T. Bradley, F. Poletti, D. J. Richardson, and R. Slavík, "How to make the propagation time through an optical fiber fully insensitive to temperature variations," *Optica* 4, no. 6, 659–668, 2017.

[10] G. T. Jasion, T. D. Bradley, K. Harrington, H. Sakr, Y. Chen, E. Numkam Fokoua, I. A. Davidson, A. Taranta, J. R. Hayes, D. J. Richardson and F. Poletti, "Hollow Core NANF with 0.28 dB/km Attenuation in the C and L Bands," in *Optical Fiber Communication Conference Postdeadline Papers 2020* paper Th4B.4.

[11] P. J. Roberts, F. Couny, H. Sabert, B. J. Mangan, D. P. Williams, L. Farr, M. W. Mason, A. Tomlinson, T. A. Birks, J. C. Knight, and P. St.J. Russell, "Ultimate low loss of hollow-core photonic crystal fibres," Opt. Express 13, 236-244 (2005)

[12] U. S. Mutugala, E. R. Numkam Fokoua, Y. Chen, T. Bradley, S. R. Sandoghchi, G. T. Jasion, R. Curtis, M. N. Petrovich, F. Poletti, D. J. Richardson and R. Slavík "Hollow-core fibers for temperature- insensitive fiber optics and its demonstration in an Optoelectronic oscillator," *Scientific Reports*, vol. 8, no. 1, pp. 1–6, 2018.

[13] M. Y. Peng, P. T. Callahan, A. H. Nejadmalayeri, S. Valente, M. Xin, L. Grüner-Nielsen, E. M. Monberg, M. Yan, J. M. Fini, and F. X. Kärtner, "Long-term stable, sub-femtosecond timing distribution via a 1.2-km polarization-maintaining fiber link: approaching 10^{-21} link stability," Opt. Express 21, 19982-19989 (2013)

[14] E. Numkam Fokoua, W. Zhu, Y Chen, S. R. Sandoghchi, T. D Bradley, M. N. Petrovich, D. J. Richardson, F. Poletti, and R. Slavík, "Polarization Effects on Thermally Stable Latency in Hollow-Core Photonic Bandgap Fibres", *in Optical Fiber Communication Conference (OFC) 2019, paper M3C.7.*

[15] C.D. Poole and J. Nagel, "Polarization effects in Lightwave systems," in *Optical Fiber Telecommunications*, eds. Kaminow, I. P. & Koch, T. L. (Academic, San Diego), Vol. IIIA, pp. 114–161 (1997)

[16] R. Motuz, "The fixed analyzer method in PMD measurement," 2016 Progress in Electromagnetic Research Symposium (PIERS), Shanghai, 2016, pp. 1794-1799.

[17] E. Numkam Fokoua, S. R. Sandoghchi, Y. Chen, G. T. Jasion, N. V. Wheeler, N. K. Baddela, J. R. Hayes, M. N. Petrovich, D. J. Richardson and F. Poletti, "Accurate modelling of fabricated hollow-core photonic bandgap fibers," Opt. Express 23, 23117-23132 (2015)

[18] F. Poletti, N. G. R. Broderick, D. J. Richardson, and T. M. Monro, "The effect of core asymmetries on the polarization properties of hollow core photonic bandgap fibers," Opt. Express 13, 9115-9124 (2005)

[19] M. Legre, M. Wegmuller, and N. Gisin, "Investigation of the Ratio Between Phase and Group Birefringence in Optical Single-Mode Fibers," J. Lightwave Technol. 21, 3374- (2003)

[20] F. Curti, B. Daino, G. De Marchis, and F. Matera, "Statistical Treatment of the Evolution of the Principal States of Polarization in Single-Mode Fibers", Journal of Lightwave Technology, Vol. 8. No. 8, pp 1162, 1990

[21] P. K. A. Wai and C. R. Menyuk, "Polarization mode dispersion, decorrelation, and diffusion in optical fibers with randomly varying birefringence," in *Journal of Lightwave Technology*, vol. 14, no. 2, pp. 148-157, Feb. 1996.

[22] C. D. Poole, J. H. Winters, and J. A. Nagel, "Dynamical equation for polarization dispersion," Opt. Lett. 16, 372-374 (1991)

[23] P. J. Roberts "Birefringent hollow core fibers", Proc. SPIE 6782, Optoelectronic Materials and Devices II, 67821R (19 November 2007);

[24] X. Chen, M.-J. Li, N. Venkataraman, M. T. Gallagher, W. A. Wood, A. M. Crowley, J. P. Carberry, L. A. Zenteno,

and K. W. Koch, "Highly birefringent hollow-core photonic bandgap fiber," Opt. Express 12, 3888-3893 (2004)

[25] J. M. Fini, J. W. Nicholson, B. Mangan, L. Meng, R. S. Windeler, E. M. Monberg, A. DeSantolo, F. V. DiMarcello and K. Mukasa, "Polarization maintaining single-mode low-loss hollow-core fibers," Nat. Commun. 5:5085 doi: 10.1038/ncomms6085 (2014).

[26] B. Zhu, B. J. Mangan, T. Kremp, G. S. Puc, V. Mikhailov, K. Dube, Y. Dulashko, M. Cortes, Y. lian, K. Marceau, B. Violette, D. Cartsounis, R. Lago, B. Savran, D. Inniss, and D. J. DiGiovanni, "First Demonstration of Hollow-Core-Fiber Cable for Low Latency Data Transmission," in Optical Fiber Communication Conference Postdeadline Papers 2020, paper Th4B.3.

[27] P. McIsaac, "Symmetry-Induced Modal Characteristics of Uniform Waveguides - I: Summary of Results," in IEEE Transactions on Microwave Theory and Techniques, vol. 23, no. 5, pp. 421-429, May 1975.

[28] G. T. Jasion, J. S. Shrimpton, Y. Chen, T. Bradley, D. J. Richardson, and F. Poletti, "MicroStructure Element Method (MSEM): viscous flow model for the virtual draw of microstructured optical fibers," Opt. Express 23, 312-329 (2015)

[29] G.T. Jasion, F. Poletti, Y. Chen, E.R. Numkam Fokoua, T.D. Bradley, "Hollow core photonic bandgap optical fibers and methods of fabrication", (2017) Patent GB2565117A

[30] Taranta, A., Numkam Fokoua, E., Abokhamis Mousavi, S. et al. Exceptional polarization purity in antiresonant hollow-core optical fibres. Nat. Photonics 14, 504–510 (2020). https://doi.org/10.1038/s41566-020-0633-x

[31] A. W. Snyder and J. D. Love, Optical Waveguide Theory (Chapman and Hall, London, 1983).

[32] D. Marcuse, Theory of Dielectric Optical waveguides, 2nd Edition (Academic Press, 1991)

[33] S.G Johnson, M. Ibanescu, M. A. Skorobogatiy, O. Weisberg, J. D. Joannopoulos, and Y. Fink, "Perturbation theory for Maxwell's equations with shifting material boundaries," Phys. Rev. E 65, 066611 (2002)